Oligomerization of the Serotonin$_{1A}$ Receptor in Live Cells: A Time-Resolved Fluorescence Anisotropy Approach

Yamuna Devi Paila,[†] Mamata Kombrabail,[‡] G. Krishnamoorthy,*[,‡] and Amitabha Chattopadhyay*[,†]

[†]Centre for Cellular and Molecular Biology, Council of Scientific and Industrial Research, Uppal Road, Hyderabad 500 007, India
[‡]Department of Chemical Sciences, Tata Institute of Fundamental Research, Homi Bhabha Road, Mumbai 400 005, India

S *Supporting Information*

ABSTRACT: The serotonin$_{1A}$ receptor is a representative member of the G-protein coupled receptor (GPCR) super-family and serves as an important target in the development of therapeutic agents for neuropsychiatric disorders. Oligomerization of GPCRs is an important contemporary issue since it is believed to be a crucial determinant for cellular signaling. In this work, we monitored the oligomerization status of the serotonin$_{1A}$ receptor tagged to enhanced yellow fluorescent protein (5-HT$_{1A}$R-EYFP) in live cells utilizing time-resolved fluorescence anisotropy decay. We interpret the unresolved fast component of the observed anisotropy decay as fluorescence resonance energy transfer (FRET) between 5-HT$_{1A}$R-EYFP molecules (homo-FRET). Homo-FRET enjoys certain advantages over hetero-FRET in the analysis of receptor oligomerization. Our results reveal the presence of constitutive oligomers of the serotonin$_{1A}$ receptor in live cells. We further show that the oligomerization status of the receptor is independent of ligand stimulation and sphingolipid depletion. Interestingly, acute (but not chronic) cholesterol depletion appears to enhance the oligomerization process. Importantly, our results are independent of receptor expression level, thereby ruling out complications arising due to high expression. These results have potential implications in future therapeutic strategies in pathophysiological conditions in which serotonin$_{1A}$ receptors are implicated.
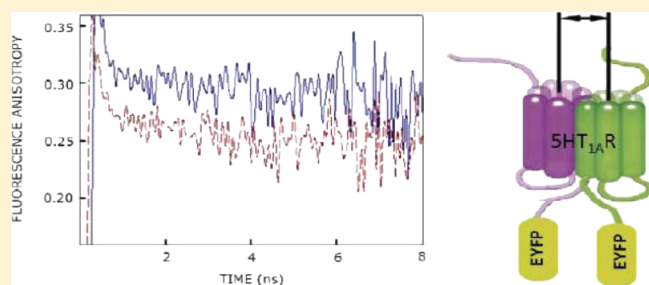
■ INTRODUCTION

The G-protein coupled receptor (GPCR) superfamily represents the largest class of molecules involved in signal transduction across the plasma membrane.[1,2] They are prototypical members of the family of seven transmembrane domain proteins and include >800 members which together constitute ~5% of the human genome.[3] GPCRs regulate physiological responses to a diverse array of stimuli and mediate multiple physiological processes. As a consequence of this, GPCRs have emerged as major targets for the development of novel drug candidates in all clinical areas.[4] It is estimated that ~50% of clinically prescribed drugs act as either agonists or antagonists of GPCRs.

Aggregation and oligomerization have often been challenging yet exciting aspects in the study of membrane proteins and receptors. The oligomerization of GPCRs represents an interesting area of contemporary receptor research[5−9] since it is believed to be an important determinant for cellular signaling. Such oligomerization is implicated in the proper folding of receptors, thereby providing the framework for efficient and controlled signal transduction. The potential implications of such oligomerization are far reaching, especially keeping in mind the role of GPCRs as major drug targets.[7]

The serotonin$_{1A}$ (5-HT$_{1A}$) receptor is an important G-protein coupled neurotransmitter receptor and is crucial in a multitude of physiological processes.[10] It serves as an important target in the

development of therapeutic agents for neuropsychiatric disorders. Interestingly, mutant (knockout) mice lacking the serotonin$_{1A}$ receptor exhibit enhanced anxiety-related behavior and represent an important animal model for genetic vulnerability to complex traits such as anxiety disorders and aggression in higher animals.[11]

In this work, we monitored the oligomerization status of the serotonin$_{1A}$ receptor tagged to enhanced yellow fluorescent protein (5-HT$_{1A}$R-EYFP) in live cells utilizing time-resolved fluorescence anisotropy decay performed in a fluorescence microscope. We interpret the observed fluorescence anisotropy decay to homo-FRET between identical fluorophores (see Results). Approaches based on fluorescence resonance energy transfer (FRET) are widely used to address oligomerization status of GPCRs in cells.[8] In most cases, energy transfer is monitored between two different fluorophores (hetero-FRET) with sufficient spectral overlap. However, hetero-FRET is often associated with a number of inherent complications, arising from the use of receptors conjugated to two different probes, and the lack of control in their relative expression levels.[12,13] Since hetero-FRET is often monitored by heterologous expression of
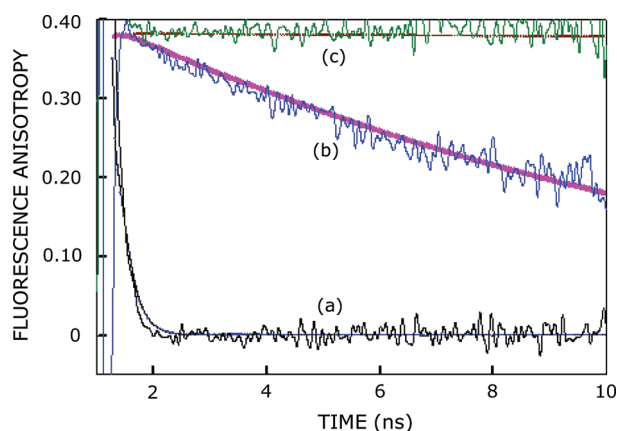
Figure 1. Time-resolved fluorescence anisotropy decay (experimental and fitted) of fluorescein in buffer (a) and soluble EYFP in buffer (b) and 80% glycerol (c). Data collection was performed in the time-resolved fluorescence microscope setup (see the Experimental Section) for validating the setup for measurements on single cells. Fits to mono-exponential anisotropy decay model are shown. The rotational correlation times estimated from the fits are 0.088 ns (a), 11.0 ns (b), and >100 ns (c). These values agree with the hydrodynamic estimates based on the molecular size and the viscosity of the medium. See the Experimental Section for other details.

proteins, the expression levels of the tagged proteins may vary, making intensity-based hetero-FRET measurements difficult to interpret. These factors have somehow limited the usefulness of FRET-based approaches in providing novel information in GPCR biology. Homo-FRET (i.e., FRET between identical fluorophores) represents a useful approach to monitor aggregation of membrane-bound molecules[14] and eliminates some of the limitations of hetero-FRET measurements. Similar to hetero-FRET, homo-FRET depends on the inverse sixth power of separation between interacting identical fluorophores on the nanometre scale and is therefore sensitive to protein oligomerization. The excitation and emission spectra of fluorophores exhibiting homo-FRET should have considerable overlap. In other words, fluorophores with relatively small Stokes' shift will have a greater probability of homo-FRET. Importantly, homo-FRET gets manifested by the genesis of a new decay process in time-resolved anisotropy decay kinetics and a resultant reduction in steady state fluorescence anisotropy, a parameter largely independent of the concentration of fluorophores,[15] and is effectively used to monitor oligomerization.[14] Homo-FRET is usually accompanied by no change in fluorescence lifetime or intensity. Our results show that the serotonin_{1A} receptor is constitutively oligomerized. In addition, we report the effects of ligand stimulation and membrane lipid (cholesterol and sphingolipid) depletion on receptor oligomerization.

■ EXPERIMENTAL SECTION

Materials. *Trans*-1,4-bis(2-dichlorobenzylaminomethyl)cyclohexane dihydrochloride (AY 9944), fumonisin B_1, methyl-β-cyclodextrin (MβCD), 8-hydroxy-2-(di-*N*-propylamino)tetralin (8-OH-DPAT), penicillin, streptomycin, gentamycin sulfate, Tris, and sodium bicarbonate were obtained from Sigma (St. Louis, MO). D-MEM/F-12 [Dulbecco's modified Eagle medium/nutrient mixture F-12 (Ham) (1:1)], fetal calf serum, and Geneticin (G 418) were from Invitrogen Life Technologies
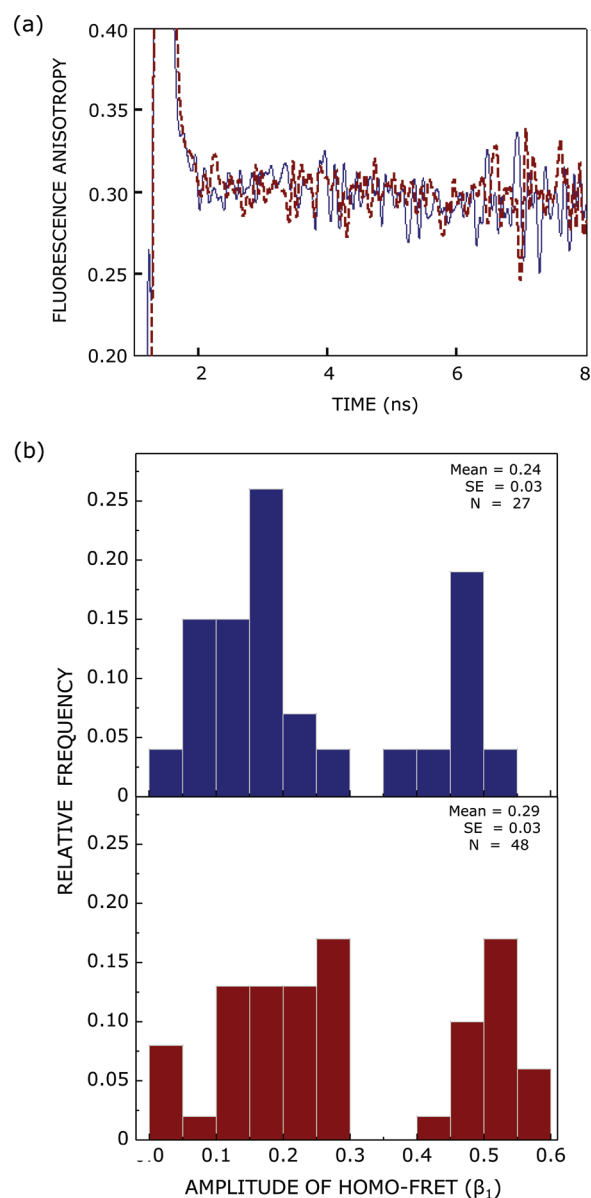

Figure 2. (a) Time-resolved fluorescence anisotropy decay of 5-HT_{1A}R-EYFP in control cells (solid line) and cells upon stimulation with 8-OH-DPAT (dashed line). EYFP was excited at 460 nm, and emission was collected using a cutoff filter of 475 nm and measured with TCSPC setup. Experiments were carried out on CHO-5-HT_{1A}R-EYFP cells in 4-(2-hydroxyethyl)-1-piperazine ethanesulfonic acid (HEPES)-Hanks buffer (pH 7.4) at room temperature (∼23 °C). (b) Frequency distribution histograms of amplitudes associated with homo-FRET of 5-HT_{1A}R-EYFP. Upper and lower parts of the panel show histograms of amplitudes associated with homo-FRET for control (untreated) cells and cells upon stimulation with 8-OH-DPAT, respectively. Means ± SE (standard error) are shown in all cases. N represents the number of independent measurements performed in each case. Apparent initial anisotropy (r_{in}^{app}) was obtained from the value of r following the initial rapid drop. The amplitude associated with homo-FRET (β_1) was estimated from the equation given in the text. See the Experimental Section for other details.

(Carlsbad, CA). Purified EYFP was a generous gift from Prof. Steven Boxer (Stanford University, CA). All other chemicals used were of the highest available purity. Water was purified

Table 1. Apparent Initial Time-Resolved Fluorescence Anisotropy of 5-HT$_{1A}$R-EYFP

condition	apparent initial fluorescence anisotropy (r_{in}^{app}) (mean ± SE)	$\beta_1{}^b$ (mean ± SE)
control^a	0.29 ± 0.011	0.24 ± 0.030
ligand (8-OH-DPAT) treated	0.27 ± 0.010	0.29 ± 0.026
control^a	0.30 ± 0.005	0.21 ± 0.014
cholesterol-depleted (acute)	0.25 ± 0.006	0.34 ± 0.016
control^a	0.32 ± 0.005	0.16 ± 0.013
cholesterol-depleted (chronic)	0.30 ± 0.007	0.21 ± 0.018
control^a	0.31 ± 0.006	0.19 ± 0.012
sphingolipid-depleted	0.31 ± 0.004	0.18 ± 0.011

^{a} For each condition, a corresponding control experiment was performed due to unavoidable day-to-day variations in r_{in}^{app}. In our data analysis, we compared r_{in}^{app} under a specific condition and the same value from the corresponding control. ^{b} Amplitude of the unresolved fast correlation time (β_1) attributed to homo-FRET (see the Supporting Information). Note that the calculated value of β_1 is in close agreement with the corresponding value obtained from the fit (see Table 2). See text for other details.

through a Millipore (Bedford, MA) Milli-Q system and used throughout.

Cells and Cell Culture. CHO-K1 cells stably expressing the serotonin$_{1A}$ receptor tagged to EYFP (referred to as CHO-5-HT$_{1A}$R-EYFP; ~10^5 receptors/cell) were used for all measurements. CHO-5-HT$_{1A}$R-EYFP cells were grown in D-MEM/F-12 (1:1) supplemented with 2.4 g/L of sodium bicarbonate, 10% fetal calf serum, 60 μg/mL penicillin, 50 μg/mL streptomycin, and 50 μg/mL gentamycin sulfate (complete medium) in a humidified atmosphere with 5% CO$_2$ at 37 °C. CHO-5-HT$_{1A}$R-EYFP cells were maintained in the above-mentioned conditions with 300 μg/mL Geneticin. Cells for fluorescence microscopy and time-resolved anisotropy measurements were grown in Lab-Tek chambered coverglass (Nunc, Denmark).

Ligand Stimulation. CHO-5-HT$_{1A}$R-EYFP cells were treated with 10 μM 8-OH-DPAT for 30 min at room temperature (~23 °C) to stimulate serotonin$_{1A}$ receptors.

Acute Cholesterol Depletion. Cells plated in Lab-Tek chambered coverglass were grown for 3 days followed by incubation in serum-free D-MEM/F-12 (1:1) medium for 3 h. Cholesterol depletion was carried out by treating cells with 10 mM MβCD in serum-free D-MEM/F-12 (1:1) medium for 30 min at 37 °C followed by a wash with serum-free D-MEM/F-12 (1:1) medium.[16]

Metabolic Depletion of Cholesterol and Sphingolipid. To achieve metabolic deprivation of cholesterol or sphingomyelin, 5 μM AY 9944 or 6 μM fumonisin B$_1$ (FB$_1$) were used, respectively.[17,18] Stock solutions of AY 9944 and FB$_1$ were prepared in water and added to cells grown for 24 h in complete medium at a final concentration of 5 μM AY 9944 or 6 μM FB$_1$ and incubated in D-MEM/F-12 medium containing 5% serum for 63−66 h. Control cells were grown under similar conditions without any treatment.

Microscopy Setup. The time-resolved fluorescence microscope was a combination of a picosecond time-resolved fluorescence spectrometer and an inverted epifluorescence microscope.[19] The time-resolved fluorescence measurements were carried out with a time-correlated single photon counting (TCSPC) setup

coupled with a picosecond laser. A titanium-sapphire picosecond laser beam (Tsunami, Spectra Physics) pumped by a diode pumped CW Nd-Vanadate laser (532 nm) (Millenia X, Spectra Physics) was used to excite EYFP at 460 nm. The pulse width of the excitation laser beam was typically ~1 ps. A pulse repetition rate of 80 MHz was reduced to a repetition rate of 4 MHz by a pulse picker. The picosecond pulses obtained after frequency doubling were guided to the objective lens by a dichroic mirror and focused onto the cells. Time-resolved fluorescence measurements were carried out on a Nikon Diaphot 300 microscope fitted with a 20× objective with 0.75 numerical aperture (NA) maintained at room temperature (~23 °C). Fluorescence emission collected by the same objective lens was passed through a cutoff filter (475 nm), a polarizer, and a pinhole placed in the image plane. Time resolution of the fluorescence signal was obtained by coupling the microscope to a TCSPC setup. The temporal resolution of the setup is ~50 ps, and the spatial resolution is ~1 μm in the xy plane. The measurements typically require ~100 fluorophore molecules in the observation volume. The instrument response function was estimated by the use of oxonol VI whose fluorescence lifetime is <50 ps. The full width at half-maximum height of the instrument response function estimated in this way was ~160 ps. Fluorophores were excited using the frequency doubled (460 nm) output of the Tsunami laser. Fluorescence emission was collected using the 475 nm bandpass filter.

In time-resolved anisotropy measurements, emission was collected at directions parallel ($I_{\parallel}$) and perpendicular ($I_{\perp}$) to the polarization of the excitation beam. Anisotropy was calculated as:

$$r(t) = \frac{I_{\parallel}(t) - I_{\perp}(t)G(\lambda)}{I_{\parallel}(t) + 2I_{\perp}(t)G(\lambda)} \tag{1}$$

where $G(\lambda)$ is the geometry factor at the wavelength λ of emission. The G factor of the emission collection optics was determined in separate experiments using a standard sample (fluorescein). Fluorescence decay curves at magic angle were analyzed by deconvoluting the observed decay with the instrument response function (IRF) to obtain the intensity decay function represented as a sum of discrete exponentials:

$$I(t) = \sum_i \alpha_i \exp(-t/\tau_i) \tag{2}$$

where $I(t)$ is the fluorescence intensity at time t and α_i is the amplitude of the ith lifetime τ_i such that $\Sigma_i\alpha_i = 1$. The time-resolved anisotropy decay was analyzed based on the model:

$$I_{\parallel}(t) = I(t)[1 + 2r(t)]/3 \tag{3}$$

$$I_{\perp}(t) = I(t)[1 - r(t)]/3 \tag{4}$$

where $I_{\parallel}(t)$ and $I_{\perp}(t)$ are the decays of the parallel (||) and perpendicular ($\perp$) components of the emission. The equation for time-resolved fluorescence anisotropy can be expressed as a biexponential decay:

$$r(t) = r_0\{\beta_1 \exp(-t/\phi_1) + \beta_2 \exp(-t/\phi_2)\} \tag{5}$$

where r_0 is the fundamental anisotropy (in case of EYFP, r_0 0.38) and β_i is the amplitude of the ith rotational correlation time ϕ_i such that $\Sigma_i\beta_i = 1$. The shorter component ϕ_1 observed in cells is due to homo-FRET between EYFP molecules, and the longer

11441

dx.doi.org/10.1021/jp201458h |*J. Phys. Chem. B* 2011, 115, 11439–11447
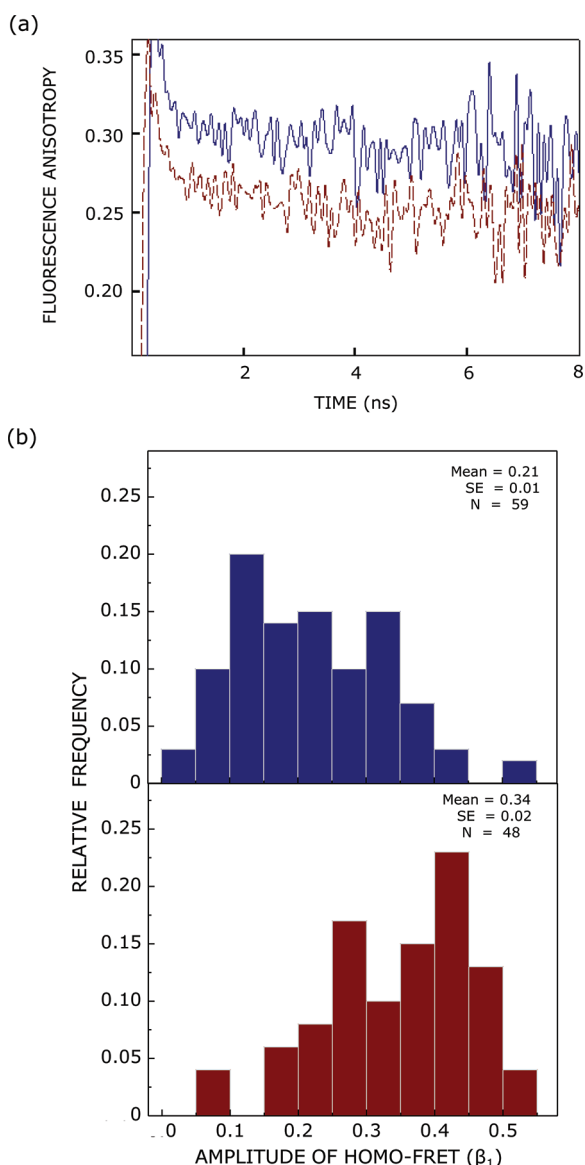
Figure 3. Time-resolved fluorescence anisotropy of 5-HT$_{1A}$R-EYFP upon acute cholesterol depletion. (a) Anisotropy decay of 5-HT$_{1A}$R-EYFP cells under control (solid line) and acute cholesterol-depleted (dashed line) conditions. (b) Frequency distribution histograms of amplitudes associated with homo-FRET of 5-HT$_{1A}$R-EYFP. Upper and lower parts of the panel show histograms of amplitudes associated with homo-FRET for control (untreated) cells and acute cholesterol-depleted cells, respectively. Acute cholesterol depletion was achieved using MβCD. Means $\pm$ SE are shown in all cases. N represents the number of independent measurements performed in each case. Apparent initial anisotropy (r_{in}^{app}) was obtained from the value of r following the initial rapid drop. The amplitude associated with homo-FRET (β_1) was estimated from the equation given in the text. All other conditions are as in Figure 2. See the Experimental Section for other details.

Figure 4. (a) Time-resolved fluorescence anisotropy decay of 5-HT$_{1A}$R-EYFP in control cells (solid line) and cells upon metabolic cholesterol depletion using AY 9944 (dashed line). (b) Frequency distribution histograms of amplitudes associated with homo-FRET of 5-HT$_{1A}$R-EYFP. Upper and lower parts of the panel show histograms of amplitudes associated with homo-FRET for control (untreated) cells and cells upon metabolic cholesterol depletion, respectively. Means $\pm$ SE are shown in all cases. N represents the number of independent measurements performed in each case. Apparent initial anisotropy (r_{in}^{app}) was obtained from the value of r following the initial rapid drop. The amplitude associated with homo-FRET (β_1) was estimated from the equation given in the text. All other conditions are as in Figure 2. See the Experimental Section for other details.

component ϕ_2 is due to restricted tumbling motion of the fluorophore.

Statistical Analysis. Frequency distribution analysis and plotting were performed using Origin software version 6.0 (OriginLab Corp., Northampton, MA). Significance levels were estimated using Student's two-tailed unpaired t-test using the same software.
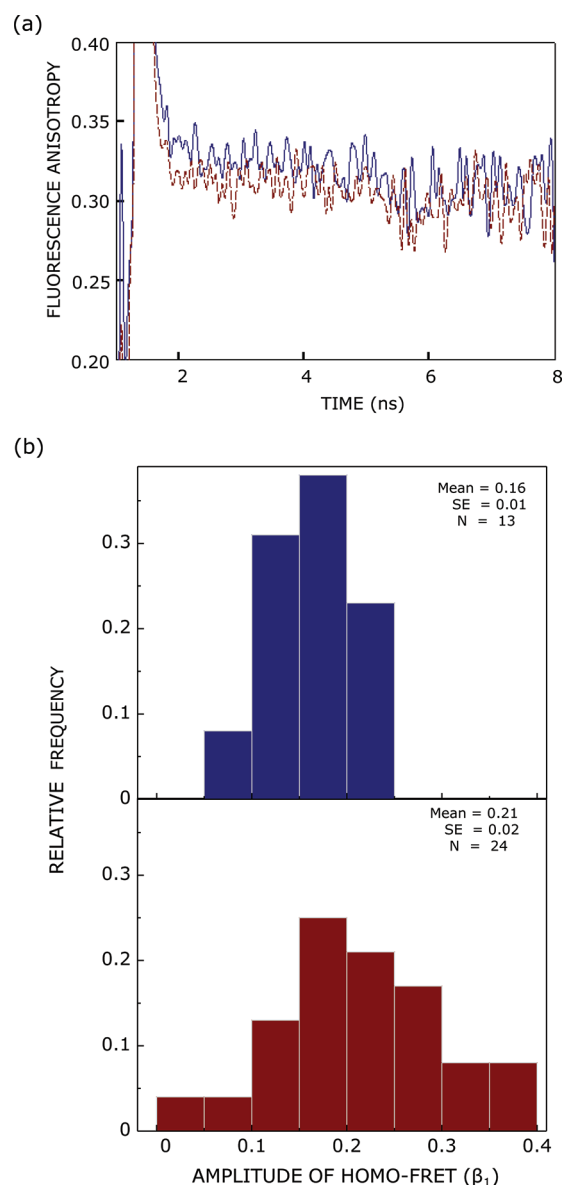
■ **RESULTS**

We have earlier characterized the heterologously expressed serotonin$_{1A}$ receptor tagged to EYFP (5-HT$_{1A}$R-EYFP) in CHO cells and shown that the tagged receptors are essentially similar to the native receptor.[20] Representative confocal images of CHO-5-HT$_{1A}$R-EYFP cells showing predominantly membrane localization of the receptor are shown in Figure 1 of the Supporting
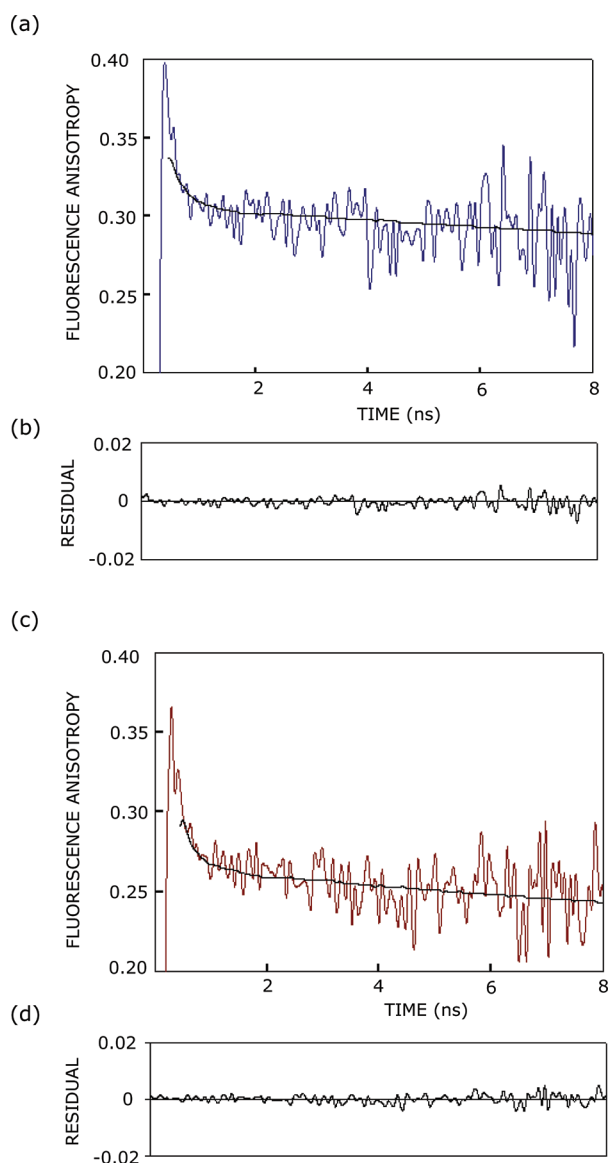
(a)

(b)

(c)

(d)

Figure 5. Time-resolved fluorescence anisotropy decay (experimental and fitted) of 5-HT$_{1A}$R-EYFP under (a) control and (c) acute cholesterol-depleted conditions. Fits to biexponential anisotropy decay model are shown. Panels b and d show the corresponding residuals. All other conditions are as in Figure 2. See the Experimental Section for other details.

Information. Polarization of emitted light could be reduced by the optical setup with high NA lenses. It has therefore been suggested that polarized FRET measurements should be limited to imaging with lenses with a numerical aperture of ≤1.0.[21] Keeping this in mind, all experiments were carried out using an objective with 0.75 NA. Preservation of polarization in the microscope setup was confirmed by the recovery of anisotropy decay kinetics of fluorescein and EYFP, wherein the fundamental anisotropy was 0.38 (see Figure 1), in agreement with the value reported earlier.[22]

Constitutive Oligomerization of the Serotonin$_{1A}$ Receptor Results in Homo-FRET. In general, the observed fluorescence anisotropy decay could be attributed to two factors: (i) homo-FRET between identical fluorophores, and (ii) rotational dynamics of fluorophores in the time scale of measurements. The rotation

of EYFP is slow due to its relatively large size and therefore does not result in depolarization of fluorescence[21] in the case of 5-HT$_{1A}$R-EYFP. For example, the rotational correlation time of EYFP in solution is ∼11 ns (Figure 1), and the fluorescence lifetime is ∼3.3 ns;[22] it is unlikely that the depolarization of emission is influenced by the rotational mobility of the fluorophore.

Figure 2 shows typical anisotropy decay curves of 5-HT$_{1A}$R-EYFP in CHO cells. The striking observation is the significant drop in the apparent value of initial (or fundamental) anisotropy (r_0) in cells compared to the observation on EYFP either in buffer or in a glycerol−water mixture (Figure 1). The small negative slope observed in the anisotropy decay curves (Figure 2) could represent the slow tumbling dynamics of EYFP on the cell membrane. The fundamental anisotropy (r_0) is an intrinsic property of a fluorophore and depends only on the angle between the absorption and the emission dipoles (transition moments). We therefore interpret the apparent reduction in anisotropy from ∼0.38 observed for EYFP in solution (Figure 1) to ∼0.31 observed for EYFP in cells (Figure 2) due to homo-FRET between EYFP molecules in proximity on the cell membrane. In turn, this would imply that the receptors are in close proximity. Apparent initial anisotropy (r_{in}^{app}) values were obtained by averaging the first few (typically 4−5) early anisotropy values after stabilization. The amplitude of the unresolved fast correlation time (β_1, see Table 1) attributed to homo-FRET was obtained using the relationship $\beta_1 = (0.38 - r_{in}^{app})/0.38$ (see Supporting Information, eq S4).

The values of the amplitude of homo-FRET (β_1) of 5-HT$_{1A}$R-EYFP are shown in Table 1 and Figures 2−4 and 6 under a given condition. The value of β_1 is ∼0.21 in cells under control conditions (this is an average value, keeping in mind day-to-day variations in β_1). A possible interpretation for this could be homo-FRET in pre-existing oligomers of the receptor due to close proximity of 5-HT$_{1A}$R-EYFP [keeping in mind the value of R_0 (the distance where FRET efficiency is 50%) for EYFP as ∼55 Å].[23,24] Interestingly, such constitutive oligomerization, a relatively new paradigm in GPCRs, has been demonstrated in case of the neurotensin receptor 1[25] and angiotensin II type 2 (AT$_2$) receptors.[26] In the case of AT$_2$ receptors, for example, constitutively active homo-oligomers have been reported to be translocated to the cell membrane and induce cell signaling, independent of receptor conformation and ligand stimulation.[26]

Agonist Stimulation. To explore the oligomerization status of the serotonin$_{1A}$ receptor upon ligand stimulation, CHO-5-HT$_{1A}$R-EYFP cells were treated with 8-OH-DPAT, which acts as a specific agonist. Figure 2a shows representative fluorescence anisotropy decay profiles of control and agonist-stimulated CHO-5-HT$_{1A}$R-EYFP cells, and the frequency distribution of β_1 is shown in Figure 2b. The value of β_1 of 5-HT$_{1A}$R-EYFP in control cells was ∼0.24, and the corresponding value upon ligand stimulation was ∼0.29 (see Table 1). These results show that there is no significant ($p > 0.05$) change in β_1 in this case, implying that there is no major change in the oligomerization status of the receptor upon agonist stimulation.

Acute but Not Metabolic Cholesterol Depletion Affects Oligomerization. We have previously shown that membrane cholesterol is required for the organization and function of the serotonin$_{1A}$ receptor.[27,28] This was shown by the depletion of membrane cholesterol either in an acute[16,29] or chronic[17,30] manner. Acute cholesterol depletion is achieved by physical depletion of cholesterol using MβCD. Acute treatment is of

11443

dx.doi.org/10.1021/jp201458h |*J. Phys. Chem. B* 2011, 115, 11439–11447

Table 2. Time-Resolved Fluorescence Anisotropy Decay Parameters of 5-HT$_{1A}$R-EYFP^a

	ϕ_1 (ns)	β_1	ϕ_2 (ns)	β_2	$r_0{}^b$	$r_{ss}{}^c$
control	0.21	0.24	155	0.76	0.388	0.298
acute cholesterol depletion (using MβCD)	0.14	0.35	105	0.65	0.390	0.254

^{a} EYFP was excited at 460 nm, and emission was collected using a cutoff filter of 475 nm and measured with the TCSPC setup. See the Experimental Section for other details. ^{b} r_0 is the fundamental anisotropy of EYFP. The value of r_0 was kept constant at 0.38[22] in the analysis. ^{c} r_{ss} is the steady state anisotropy, obtained by integration of the area under the time-resolved anisotropy decay curve.

relatively short duration. On the other hand, metabolic (chronic) depletion of cholesterol is generally achieved using inhibitors of cholesterol biosynthesis such as statin[30] or AY 9944.[17] Metabolic cholesterol depletion takes place over a longer period of time and represents a *chronic* treatment, thereby mimicking physiological situations.

Typical anisotropy decays of control and acute cholesterol-depleted CHO-5-HT$_{1A}$R-EYFP cells are shown in Figure 3. The value of β_1 of 5-HT$_{1A}$R-EYFP exhibits significant ($p < 0.001$) increase upon treatment with MβCD to ~0.34 (Table 1 and Figure 3b). These results imply that there is a possible reorganization of the receptor upon acute cholesterol depletion, resulting in an increase in oligomerization status. This is in agreement with our previous results that acute cholesterol depletion using MβCD induces possible reorganization of the receptor into ordered domains and results in confined diffusion of the receptor.[16,31] On the other hand, the value of β_1 shows no significant ($p > 0.05$) change upon metabolic (chronic) cholesterol depletion (see Table 1 and Figure 4b) using AY 9944, a distal inhibitor of cholesterol biosynthesis.[17] This implies that metabolic cholesterol depletion does not lead to a major change in the oligomerization of the receptor. An interesting aspect of these results is that oligomerization status of the serotonin$_{1A}$ receptor appears to depend on the manner in which cholesterol depletion is carried out. This could be due to the time available for the receptor to reorganize in case of metabolic depletion. Acute cholesterol depletion is quick and therefore may not provide sufficient time to the receptor for extensive reorganization.

Because of the significant increase in β_1 upon acute cholesterol depletion, we carried out further detailed analysis of these results. The time-resolved fluorescence anisotropy decay of 5-HT$_{1A}$R-EYFP in control and acute cholesterol-depleted conditions are shown in Figure 5. The decays could be fitted to a sum of two exponentials using eq 5. The biexponential fits and the statistical parameters used to check the goodness of the fit are shown in Figure 5. The corresponding rotational correlation times (ϕ) from the analysis of the fitted anisotropy decays are shown in Table 2. As mentioned above, the shorter component ϕ_1 corresponds to homo-FRET. This decay rate is a sensitive measure of the distance between fluorophores involved in homo-FRET with faster decay rates indicating shorter intermolecular distances.[32] Our results show that the value of ϕ_1 is reduced upon acute cholesterol depletion, suggesting that the distance between 5-HT$_{1A}$R-EYFP is reduced, implying that the receptor gets reorganized to more numbers of oligomers (or higher order oligomers) upon acute cholesterol depletion. The amplitude of homo-FRET (β_1) under various conditions is also shown in Table 1. The table shows that maximum homo-FRET takes place under acute cholesterol-depleted conditions, as indicated by the difference in β_1 between control and treatment conditions. Importantly, the calculated value of β_1 (in Table 1) is in close agreement with the corresponding value obtained from the fit

(see Table 2) in the case of control and acute cholesterol-depleted conditions. This self-consistency in the values of β_1 validates the framework shown in the Supporting Information. This further reinforces the proposal of reorganization of serotonin$_{1A}$ receptors to higher oligomers upon acute cholesterol depletion. In addition, the considerable reduction (~15%) in steady state anisotropy (r_{ss}) supports that the oligomerization state of the receptor is enhanced upon acute cholesterol depletion (Table 2).

Sphingolipid Depletion Does Not Alter the Oligomerization of the Serotonin$_{1A}$ Receptor. Sphingolipids are essential components of eukaryotic cell membranes and are involved in a variety of cellular functions. We modulated sphingolipid levels in CHO-5-HT$_{1A}$R-EYFP cells by metabolically inhibiting the biosynthesis of sphingolipids using fumonisin B$_1$ (FB$_1$).[18] Figure 6a shows representative fluorescence anisotropy decay profiles of control and sphingolipid-depleted CHO-5-HT$_{1A}$R-EYFP cells, and the frequency distribution of β_1 is shown in Figure 6b. Table 1 shows that the value of β_1 remains invariant upon metabolic sphingolipid depletion, indicating that there is no major change in the oligomerization status of the receptor upon sphingolipid depletion.

Oligomerization Is Independent of Receptor Expression Level. Oligomerization of membrane proteins can be induced by trivial association due to overexpression of a given protein. For example, it has been previously reported that the neurokinin-1 receptor may appear to oligomerize at higher expression levels but is monomeric at low levels of expression.[13] To avoid such complications, we analyzed the dependence of β_1 on receptor expression levels. The value of β_1 obtained from cells at varying fluorescence intensities are shown in Figure 7. The figure contains data with receptors differing in expression levels by ~12-fold, since a similar fold change in fluorescence intensity is observed. Importantly, the absence of any specific trend in the scatter shows that the measured anisotropies were independent of receptor expression level. We therefore conclude that the oligomeric status of the serotonin$_{1A}$ receptor reported by us is independent of the receptor expression level.

■ DISCUSSION

There are a few studies describing the oligomerization of serotonin$_{1A}$ receptors.[33−35] However, these studies were based on either hetero-FRET[34,35] or coimmunoprecipitation.[33] As mentioned above, while hetero-FRET suffers from a number of limitations, immunological approaches are susceptible to cross-reactivity. In the present work, we utilized homo-FRET that is free from these limitations and monitored the oligomerization state of the serotonin$_{1A}$ receptor in live cells utilizing time-resolved fluorescence anisotropy decay measurements. From the observed change in the amplitude of homo-FRET (β_1), we propose the presence of constitutive oligomers of the serotonin$_{1A}$
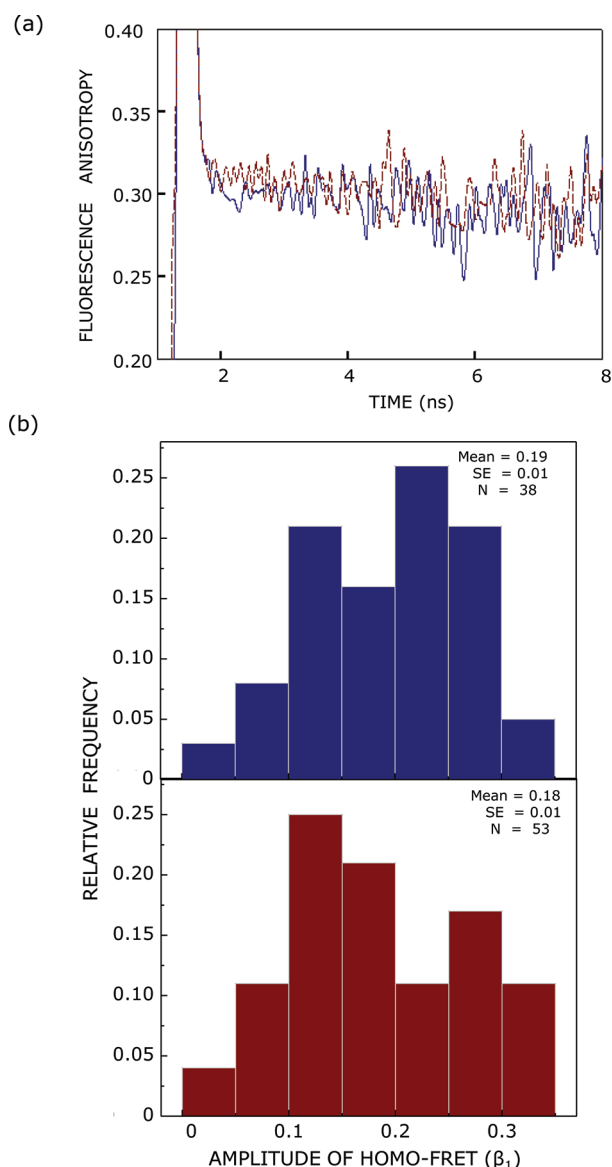
(a)

(b)

Figure 7. Apparent initial anisotropy (r_{in}^{app}) values of 5-HT$_{1A}$R-EYFP are independent of fluorescence intensity of 5-HT$_{1A}$R-EYFP. Anisotropy values from a large ($N > 45$) number of measurements plotted against the corresponding fluorescence intensity. These measurements were carried out by moving the focused laser beam to different locations within a cell or different cells showing different brightness. It is apparent that there is no systematic variation of anisotropy with intensity. All other conditions are as in Figure 2. See the Experimental Section for other details.

Figure 6. Time-resolved fluorescence anisotropy of 5-HT$_{1A}$R-EYFP upon sphingolipid depletion. (a) Anisotropy decay of 5-HT$_{1A}$R-EYFP cells under control (solid line) and sphingolipid-depleted (dashed line) conditions. Sphingolipid depletion was achieved using FB$_1$. (b) Frequency distribution histograms of amplitudes associated with homo-FRET of 5-HT$_{1A}$R-EYFP. Upper and lower parts of the panel show histograms of amplitudes associated with homo-FRET for control (untreated) cells and sphingolipid-depleted cells, respectively. Means $\pm$ SE are shown in all cases. N represents the number of independent measurements performed in each case. Apparent initial anisotropy (r_{in}^{app}) was obtained from the value of r following the initial rapid drop. The amplitude associated with homo-FRET (β_1) was estimated from the equation given in the text. All other conditions are as in Figure 2. See the Experimental Section for other details.

receptor. We show that the oligomerization status of the receptor is independent of ligand stimulation and sphingolipid depletion. Importantly, acute (but not chronic) cholesterol depletion appears to enhance the oligomerization process.

We previously monitored the oligomerization status of the serotonin$_{1A}$ receptor in live cells using homo-FRET.[14c] Our previous work was based on increase in steady state anisotropy
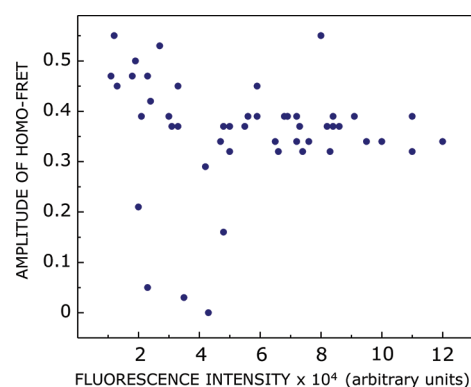
upon photobleaching under different conditions. The variation in the value of steady state anisotropy was interpreted as indicative of variation in the level of homo-FRET and therefore the level of oligomerization. While this interpretation is generally accepted, a far more direct way to assess the level of homo-FRET is by directly measuring the amplitude (β_1 in this work) associated with the homo-FRET component in direct time-resolved anisotropy measurements. While the present measurements are technically far more demanding, they offer unequivocal evidence for the change in the level of homo-FRET. This is because interpretation of variation in steady state anisotropy as representing the variation in the level of homo-FRET assumes that other rotational dynamic components do not vary, an assumption that is not checked during steady state measurements.

An interesting aspect of our results is that, while acute cholesterol depletion appears to enhance the oligomerization of the serotonin$_{1A}$ receptor, metabolic depletion does not influence the receptor oligomerization in a major way. Cholesterol is known to modulate lipid−protein interactions by increasing the thickness of the membrane lipid bilayer. For example, it has been shown that the membrane bilayer thickness in vesicles of 1-palmitoyl-2-oleoyl-sn-glycero-3-phosphocholine (POPC) is ∼26 Å which increases to 30 Å in presence of 30 mol % cholesterol.[36] This can give rise to "hydrophobic mismatch", that is, a difference in the hydrophobic lengths of transmembrane proteins and the surrounding lipid annulus, that can lead to changes in membrane protein conformation[37] and oligomerization.[38] In situations of hydrophobic mismatch, when the energetic cost of membrane deformation is high,[39] transmembrane proteins and receptors may respond by forming lateral aggregates (oligomers) that would reduce the membrane-exposed surface. Acute cholesterol depletion may result in such hydrophobic mismatch-like situation leading to increased oligomerization of the receptor. This may not be true in case where cholesterol depletion is carried out using inhibitors of cholesterol biosynthesis (chronic depletion), since extensive membrane reorganization could take place (thereby preventing hydrophobic mismatch) due to longer duration of the process.

Our results have potential implications in drug design and development in pathophysiological conditions in which serotonin$_{1A}$ receptors are implicated.[40] Homo- and hetero-oligomerization of GPCRs assume greater significance in the pharmacology of GPCRs since oligomerization gives rise to pharmacological diversity,[41] opening new avenues for therapeutics. Oligomerization of GPCRs also offers an attractive mechanism for increasing the diversity of cellular responses to extracellular signals or stimuli. In view of the enormous implications of GPCR function in human health, progress in our understanding of the oligomerization status of GPCRs would enhance our ability to design better therapeutic strategies to combat diseases related to malfunctioning of these receptors.

■ ASSOCIATED CONTENT

ⓢ Supporting Information. Representative images of CHO cells (supplementary Figure 1) and a further explanation of the calculation of β_1 values seen in Table 1 of the text. This material is available free of charge via the Internet at http://pubs.acs.org.

■ AUTHOR INFORMATION

Corresponding Author

*Address correspondence to Amitabha Chattopadhyay, Centre for Cellular & Molecular Biology, Uppal Road, Hyderabad 500 007, India. Tel.: +91-40-2719-2578; fax: +91-40-2716-0311; e-mail: amit@ccmb.res.in; or G. Krishnamoorthy, Department of Chemical Sciences, Tata Institute of Fundamental Research, Homi Bhabha Road, Mumbai 400 005, India. Tel.: +91-22-2278-2301; fax: +91-22-2280-4610; e-mail: gk@tifr.res.in.

■ ACKNOWLEDGMENT

■ REFERENCES

(1) Pierce, K. L.; Premont, R. T.; Lefkowitz, R. J. *Nat. Rev. Mol. Cell Biol.* **2002**, *3*, 639–650.

(2) Rosenbaum, D. M.; Rasmussen, S. G. F.; Kobilka, B. K. *Nature* **2009**, *459*, 356–363.

(3) Zhang, Y.; DeVries, M. E.; Skolnick, J. *PLoS Comput. Biol.* **2006**, *2*, 88–99.

(4) Heilker, R.; Wolff, M.; Tautermann, C. S.; Bieler, M. *Drug Discovery. Today* **2009**, *14*, 231–240.

(5) Shanti, K.; Chattopadhyay, A. *Curr. Sci.* **2000**, *79*, 402–403.

(6) Park, P. S.; Filipek, S.; Wells, J. W.; Palczewski, K. *Biochemistry* **2004**, *43*, 15643–15656.

(7) Milligan, G. *Drug Discovery Today* **2006**, *11*, 541–549.

(8) Lohse, M. J. *Curr. Opin. Pharmacol.* **2009**, *10*, 53–58.

(9) Palczewski, K. *Trends Biochem. Sci.* **2010**, *35*, 595–600.

(10) (a) Pucadyil, T. J.; Kalipatnapu, S.; Chattopadhyay, A. *Cell. Mol. Neurobiol.* **2005**, *25*, 553–580. (b) Kalipatnapu, S.; Chattopadhyay, A. *Cell. Mol. Neurobiol.* **2007**, *27*, 1097–1116.

(11) Gardier, A. M. *Behav. Pharmacol.* **2009**, *20*, 18–32.

(12) James, J. R.; Oliveira, M. I.; Carmo, A. M.; Iaboni, A.; Davis, S. J. *Nat. Methods* **2006**, *3*, 1001–1006.

(13) Meyer, B. H.; Segura, J.-M.; Martinez, K. L.; Hovius, R.; George, N.; Johnsson, K.; Vogel, H. *Proc. Natl. Acad. Sci. U.S.A.* **2006**, *103*, 2138–2143.

(14) (a) Varma, R.; Mayor, S. *Nature* **1998**, *394*, 798–801. (b) Sharma, P.; Varma, R.; Sarasij, R. C.; Ira; Gousset, K.; Krishnamoorthy, G.; Rao, M.; Mayor, S. *Cell* **2004**, *116*, 577–589. (c) Ganguly, S.; Clayton, A. H. A.; Chattopadhyay, A. *Biophys. J.* **2011**, *100*, 361–368.

(15) Tramier, M.; Piolot, T.; Gautier, I.; Mignotte, V.; Coppey, J.; Kemnitz, K.; Durieux, C.; Coppey-Moisan, M. *Methods Enzymol.* **2003**, *360*, 580–597.

(16) Pucadyil, T. J.; Chattopadhyay, A. *Biochim. Biophys. Acta* **2007**, *1768*, 655–668.

(17) Paila, Y. D.; Murty, M. R. V. S.; Vairamani, M.; Chattopadhyay, A. *Biochim. Biophys. Acta* **2008**, *1778*, 1508–1516.

(18) Paila, Y. D.; Ganguly, S.; Chattopadhyay, A. *Biochemistry* **2010**, *49*, 2389–2397.

(19) Srivastava, A.; Krishnamoorthy, G. *Arch. Biochem. Biophys.* **1997**, *340*, 159–167.

(20) Pucadyil, T. J.; Kalipatnapu, S.; Harikumar, K. G.; Rangaraj, N.; Karnik, S. S.; Chattopadhyay, A. *Biochemistry* **2004**, *43*, 15852–15862.

(21) Piston, D. W.; Kremers, G. J. *Trends Biochem. Sci.* **2007**, *32*, 407–414.

(22) Borst, J. W.; Hink, M. A.; van Hoek, A.; Visser, A. J. W. G. *J. Fluoresc.* **2005**, *15*, 153–160.

(23) Patterson, G. H.; Piston, D. W.; Barisas, B. G. *Anal. Biochem.* **2000**, *284*, 438–440.

(24) Ganesan, S.; Ameer-beg, S. M.; Ng, T. T. C.; Vojnovic, B.; Wouters, F. S. *Proc. Natl. Acad. Sci. U.S.A.* **2006**, *103*, 4089–4094.

(25) Harding, P. J.; Attrill, H.; Boehringer, J.; Ross, S.; Wadhams, G. H.; Smith, E.; Armitage, J. P.; Watts, A. *Biophys. J.* **2009**, *96*, 964–973.

(26) Miura, S.; Karnik, S. S.; Saku, K. *J. Biol. Chem.* **2005**, *280*, 18237–18244.

(27) Pucadyil, T. J.; Chattopadhyay, A. *Prog. Lipid Res.* **2006**, *45*, 295–333.

(28) (a) Paila, Y. D.; Chattopadhyay, A. *Subcell. Biochem.* **2010**, *51*, 439–466. (b) Saxena, R.; Chattopadhyay, A. *J. Neurochem.* **2011**, *116*, 726–733.

(29) Pucadyil, T. J.; Chattopadhyay, A. *Biochim. Biophys. Acta* **2004**, *1663*, 188–200.

(30) Shrivastava, S.; Pucadyil, T. J.; Paila, Y. D.; Ganguly, S.; Chattopadhyay, A. *Biochemistry* **2010**, *49*, 5426–5435.

(31) Kalipatnapu, S.; Chattopadhyay, A. *Mol. Membr. Biol.* **2005**, *22*, 539–547.

(32) Gautier, I.; Tramier, M.; Durieux, C.; Coppey, J.; Pansu, R. B.; Nicolas, J.-C.; Kemnitz, K.; Coppey-Moisan, M. *Biophys. J.* **2001**, *80*, 3000–3008.

(33) Salim, K.; Fenton, T.; Bacha, J.; Urien-Rodriguez, H.; Bonnert, T.; Skynner, H. A.; Watts, E.; Kerby, J.; Heald, A.; Beer, M.; McAllister, G.; Guest, P. C. *J. Biol. Chem.* **2002**, *277*, 15482–15485.

(34) Łukasiewicz, S.; Błasiak, E.; Faron-Górecka, A.; Polit, A.; Tworzydło, M.; Górecki, A.; Wasylewski, Z.; Dziedzicka-Wasylewska, M. *Pharmacol. Rep.* **2007**, *59*, 379–392.

(35) Kobe, F.; Renner, U.; Woehler, A.; Wlodarczyk, J.; Papusheva, E.; Bao, G.; Zeug, A.; Richter, D. W.; Neher, E.; Ponimaskin, E. *Biochim. Biophys. Acta* **2008**, *1783*, 1503–1516.

(36) Nezil, F. A.; Bloom, V. *Biophys. J.* **1992**, *61*, 1176–1183.

(37) (a) Jensen, M. Ø.; Mouritsen, O. G. *Biochim. Biophys. Acta* **2004**, *1666*, 205–226. (b) Kelkar, D. A.; Chattopadhyay, A. *Biochim. Biophys. Acta* **2007**, *1768*, 1103–1113.

11446

dx.doi.org/10.1021/jp201458h |*J. Phys. Chem. B* 2011, 115, 11439–11447

(38) Ge, M.; Freed, J. H. *Biophys. J.* **1999**, *76*, 264–280.

(39) Lundbæk, J. A.; Andersen, O. S.; Werge, T.; Nielsen, C. *Biophys. J.* **2003**, *84*, 2080–2089.

(40) Akimova, E.; Lanzenberger, R.; Kasper, S. *Biol. Psychiatry* **2009**, *66*, 627–635.

(41) Terrillon, S.; Bouvier, M. *EMBO Rep.* **2004**, *5*, 30–34.

11447

dx.doi.org/10.1021/jp201458h |*J. Phys. Chem. B* 2011, 115, 11439–11447